

DECARBURIZATION OF NON-ORIENTED ELECTRICAL STEEL SHEETS DOPED WITH SELENIUM

RAZOGLJIČENJE NEORIENTIRANE ELEKTROPLOČEVINE, LEGIRANE S SELENOM

Darja Steiner Petrovič¹, Monika Jenko¹, Hans Jürgen Grabke², Vasilij Prešern³

¹ Institute of Metals and Technology, Lepi pot 11, 1000 Ljubljana, Slovenija

² Max-Planck-Institut für Eisenforschung, Max-Planck-Straße 1, Düsseldorf, Germany

³ ACRONI d.o.o., Cesta Borisa Kidriča 44, 4270 Jesenice, Slovenija
darja.steiner@imt.si

Prejem rokopisa - received: 2001-10-26; sprejem za objavo - accepted for publication: 2002-01-17

Gas-metal reactions like decarburization annealing are affected by the temperature, the composition of the metal surface and the gas mixture. During annealing, interactions take place among the atoms on the steel's surface, those from the gas phase, as well as dissolved atoms from the bulk and segregated atoms. Several authors have reported that selenium improves the magnetic properties of grain-oriented electrical steel sheets. The effect of 0,05 mas. % of Se on the decarburization of non-oriented silicon steel sheet has been investigated in this study.

Key words: non-oriented electrical steel sheets, decarburization, recrystallization, non-metallic inclusions, selenium

Kemijske reakcije na fazni meji plin-kovina, npr. razogljčenje, so odvisne od temperature, kemijske sestave kovinske površine in plinske mešanice. Na površini jekla med žarjenjem nastajajo interakcije med atomi iz plinske faze, raztopljenimi atomi iz trdne raztopine in segregiranimi atomi iz jekla. Različni raziskovalci poročajo, da selen izboljšuje magnetne lastnosti orientiranih elektropločevin. V tej raziskavi smo preučevali vpliv 0,05 mas. % Se na razogljčenje neorientirane elektropločevine.

Ključne besede: neorientirana elektropločevina, razogljčenje, rekristalizacija, nekovinski vključki, selen

1 INTRODUCTION

In the production of grain-oriented and non-oriented electrical steel sheets special attention is paid to the recrystallization and the development of texture. In grain-oriented steel it is the Goss texture (110) that is preferred, and this type of texture is obtained by a secondary recrystallization. Much less is known about the parameters influencing texture development in non-oriented electrical steels, where the most appropriate form of texture is a cubic texture in which grains have their (001) plane lying parallel to the plane of the sheet.

In the processing of grain-oriented and non-oriented electrical steel sheets some alloying elements such as Si and Al are added to increase the electrical resistivity and, hence, to decrease the eddy-current losses.^{1,2} The presence of Al and Mn can be observed in the microstructure as AlN and MnS inclusions. In the grain-oriented steels, AlN and MnS particles are used as inhibitors of the secondary recrystallization. In earlier studies of non-metallic inclusions in steels^{3,4} it was observed that MnS inclusions in a range of different steels sometimes contained other transition elements - Ti, V, Cr, Fe, Co, Ni, Se - in a substitutional solid solution. It was also reported that Se improved the machinability of manganese steel⁵, case-hardened steel⁶ and free-cutting steel.⁷ In the deep drawing steel sheets the selenide-sulphide inclusions influence the recrystallization and therefore the development of the

texture. Selenium doping was found to be especially beneficial for the development of texture, the anisotropy and the drawability of deep-drawing steel.⁸

The texture and desirable magnetic properties of grain-oriented and non-oriented electrical steels are strongly dependent on carbon content as well, and therefore a decarburization stage for these steels is one of the most important phases in the production.

2 EXPERIMENTAL

The chemical composition of the investigated steels is given in **Table 1**. The samples used in this study were 1,5-mm-thick cold-rolled sheets. The samples were decarburized in a mixture of hydrogen and water vapor (H₂-H₂O) at 840 °C. The dew points of the gas mixture were T_{H₂O} = 25 °C, 40 °C and 50 °C, corresponding to p(H₂O)/p(H₂) = 0,03, 0,07 and 0,12 respectively. After decarburization the samples were cooled in helium to room temperature. The residual carbon content after the decarburization was determined by chemical analysis and the microstructure of the steels after decarburization was investigated by optical microscopy. Samples were metallographically prepared by grinding, polishing and etching.

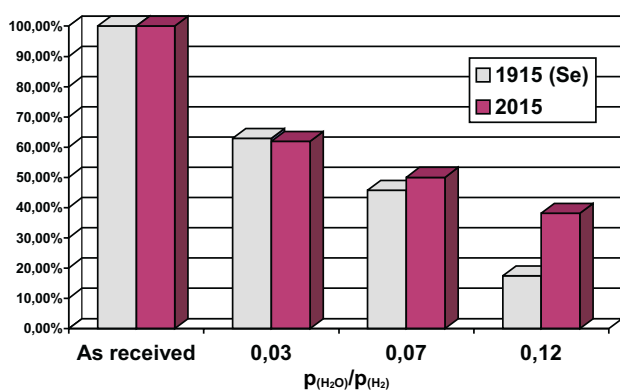
For the surface analysis of the oxide layers some of the samples were encapsulated in glass test tubes containing a protective gas to prevent any further surface reactions. An analysis using HRAES (high-resolution

Table 1: Chemical composition of the investigated steels (mas. %)**Tabela 1:** Kemijska sestava preiskovanih jekel (mas. %)

Sample	% C	% Si	% Al	% Mn	% Cu	% P	% S	% Se
1915	0,035	1,7	0,83	0,2	0,015	0,0029	0,0028	0,050
2015	0,042	1,7	0,85	0,2	0,010	0,0022	0,0020	-

Table 2(a): Residual carbon content (in mas. %) after decarburization in a wet hydrogen at 840 °C for 15 minutes**Tabela 2(a):** Preostala koncentracija ogljika po 15-minutnem razogljčenju v vlažnem vodiku pri temperaturi 840 °C

Sample	As received	$p(\text{H}_2\text{O})/p(\text{H}_2)$		
		0,03	0,07	0,12
1915 (Se)	0,035 mas. % (100 %)	0,022 mas. % (62,85 %)	0,016 mas. % (45,71 %)	0,0061 mas. % (17,42 %)
2015	0,042 mas. % (100%)	0,026 mas. % (61,9 %)	0,021 mas. % (50 %)	0,0160 mas. % (38,1 %)

**Table 2(b):** Residual carbon content (percentage of the initial amount) after decarburization in a wet hydrogen at 840 °C for 15 minutes**Tabela 2(b):** Preostali delež ogljika glede na izhodno vrednost po 15-minutnem razogljčenju v vlažnem vodiku pri temperaturi 840 °C

Auger-electron spectroscopy) of the steel sheets' surfaces and cross-sections was performed. Oxide layers were investigated in the as-received condition in a UHV using SEM and HRAES. Additional HRAES measurements were made after argon-ion sputtering. Metallographically ground and polished cross-sections were also investigated by SEM and HRAES. The adsorbed impurities on the surface of the cross-sections were removed by cleaning with argon-ion sputtering.

3 RESULTS AND DISCUSSION

The residual carbon content after decarburization of the steel sheets is given in table 2. The carbon content after decarburization in wet hydrogen at 840 °C and $p(\text{H}_2\text{O})/p(\text{H}_2) = 0,03$ for 15 minutes was almost the same for steel doped with selenium and steel without any selenium addition. The micrographs in Figure 1 show that the microstructure of both steels consisted of ferrite grains. The recrystallization in the steel sheet containing selenium after decarburizing annealing was incomplete (**Figure 1a**), while the grains in the selenium-free steel were completely recrystallized. (The difference in the

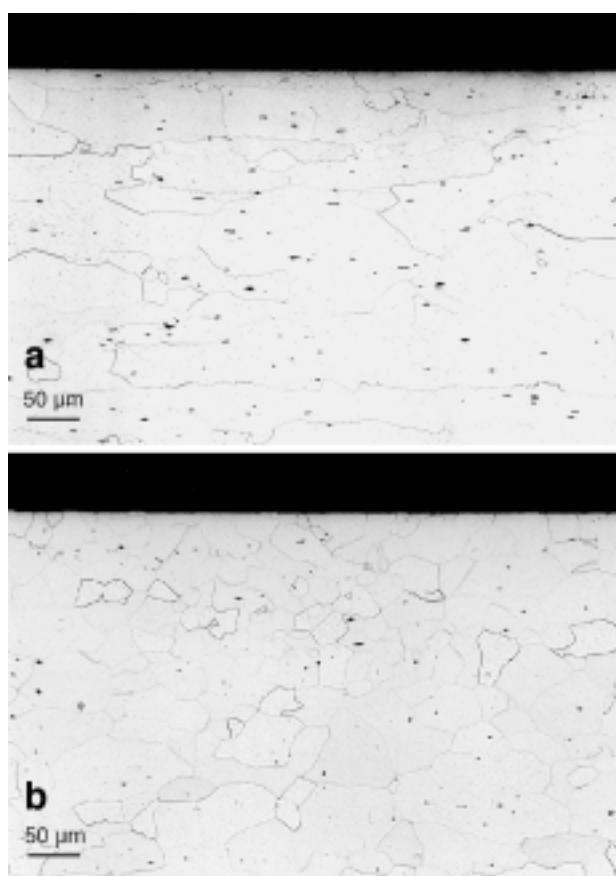


Figure 1: Microstructure of the samples after decarburization in a wet hydrogen at 840 °C; $p(\text{H}_2\text{O})/p(\text{H}_2) = 0,03$, $t = 15$ minutes (Etchant: Nital); (a) sample 1915 with Se; (b) sample 2015 - comparison steel
Slika 1: Mikrostruktura jeklene pločevine po razogljčenju pri 840 °C v vlažnem vodiku; $p(\text{H}_2\text{O})/p(\text{H}_2) = 0,03$, $t = 15$ minut (jedkalo: nital); (a) vzorec 1915 s Se; (b) vzorec 2015 - primerjalno jeklo

recrystallization behavior of the selenium-doped and the selenium-free steel sheets is even more obvious from the comparison of the microstructures in **Figure 2**). In the microstructure of the steel sheet 1915, with 0,05 mas. % Se, the rolling grain shape can still be distinguished (**Figure 1a**). The retained rolling texture in the

non-oriented electrical steels can be explained in terms of a stored-energy-dependent nucleation mechanism.^{2,8} On the other hand, the grains of the steel 2015 are polyhedral (**Figure 1b**). It is evident from the microstructure that the steel with the selenium addition contains more non-metallic inclusions, which are coarser and are elongated in parallel with the rolling direction (**Figure 1a**).

The decarburization with $p(\text{H}_2\text{O})/p(\text{H}_2) = 0,07$ and $p(\text{H}_2\text{O})/p(\text{H}_2) = 0,12$ was more efficient with sample 1915, which contains selenium (**Table 2 a, b**). The shape of the crystal grains in **Figure 2a** indicates an abnormal grain growth beneath the surface, where the steel was decarburized more effectively. Below the region of abnormal grain growth in the microstructure of this steel sheet an incompletely recrystallized region is observed. The recrystallized grains in the steel 2015 are smaller, polyhedral and more homogenous in size (**Figure 2b**). An incomplete recrystallization was also observed in non-oriented electrical steel that was alloyed with antimony.⁹ The delayed recrystallization in antimony-containing steel sheet was explained by the longer incubation time of some recrystallization nuclei.

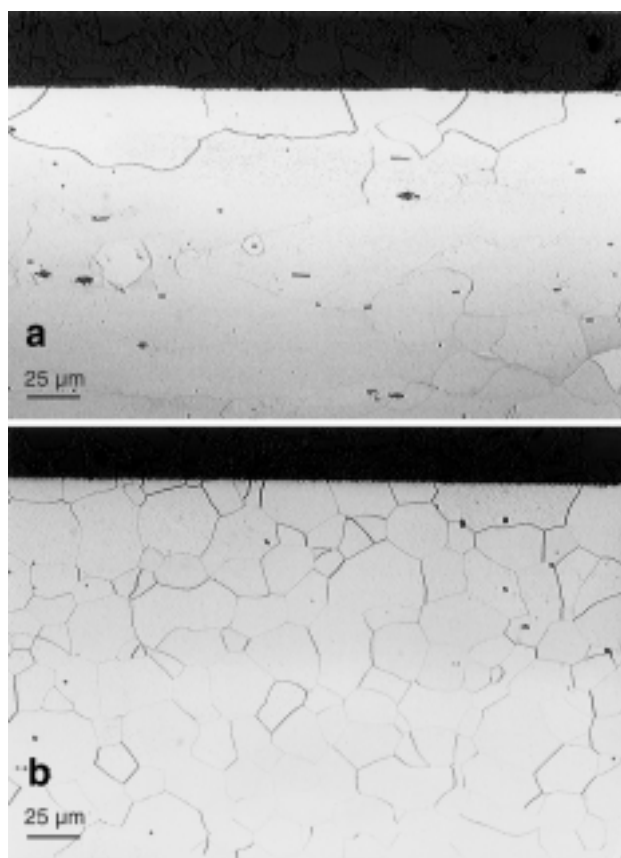


Figure 2: Microstructure of the samples after decarburization in a wet hydrogen at 840 °C; $p(\text{H}_2\text{O})/p(\text{H}_2) = 0,07$, $t = 15$ minutes (Etchant: Nital); (a) sample 1915 with Se; (b) sample 2015 - comparison steel
Slika 2: Mikrostruktura jeklene pločevine po razogljichenju pri 840 °C v vlažnem vodiku; $p(\text{H}_2\text{O})/p(\text{H}_2) = 0,07$, $t = 15$ minut (jedkalo: nital); (a) vzorec 1915 s Se; (b) vzorec 2015 - primerjalno jeklo

In **Figure 3a** there is a SEM image of a complex non-metallic inclusion in the steel 1915. The inclusion shown in this figure is elongated in the rolling direction and it is approximately 8 µm long. At the position P3 there is a coarse and angular-shaped AlN particle. In this complex non-metallic inclusion sulphur was found at the positions P1 and P4. The AES sulphur peaks are indicated on the spectra P1 and P4 in **Figure 3b**. Selenium and copper enrichments were found in the elongated part of the inclusion at positions P1, P2 and P4. The spectra P1, P2 and P4 in **Figure 3b** show the AES peaks for selenium and copper. In an investigation of relevant literature we could not find any reports of the co-existence of selenium and copper in non-metallic inclusions.

The elongated part of the complex inclusion in **Figure 3a**, where AES measurements at the positions P1, P2 and P4 were made, seems to have a selenide or selenide-sulphide structure. In the (Mn,Se)S-type sulphide inclusions, selenium atoms are substitute for those of manganese. In the AES spectra it is difficult to distinguish among Mn-LM2, Mn-LM1, Fe-LM6 and Fe-LM4 peaks. Therefore, from AES spectra P1 and P4

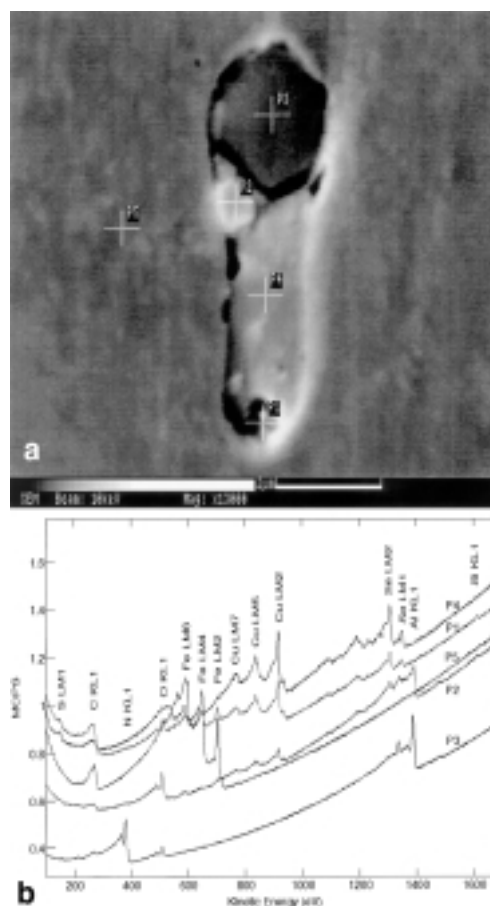


Figure 3: (a) SEM image of a non-metallic inclusion. (b) AES spectra at positions P1-P5

Slika 3: (a) SEM-posnetek nekovinskega vključka. (b) AES-spektri na mestih P1-P5

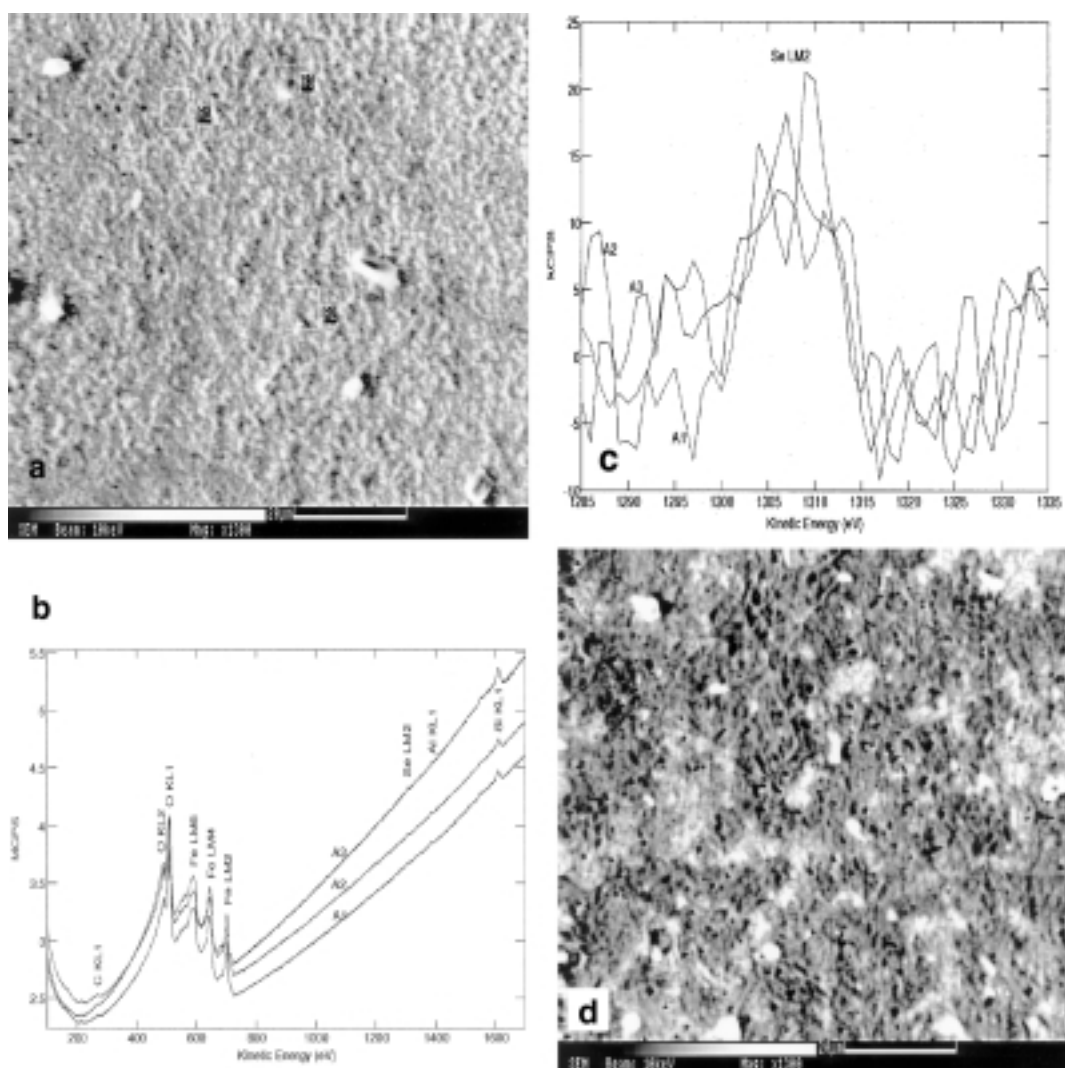


Figure 4: The oxidized surface after decarburization in wet hydrogen; $p(\text{H}_2\text{O})/p(\text{H}_2) = 0,12$. (a) SEM image of the sample 1915 with Se; (b) AES spectra of the areas A1, A2 and A3; (c) AES peaks of Se with subtracted backgrounds (d) SEM image of the sample 2015

Slika 4: Oksidirana površina jekla po razogljichenju v vlažnem vodik; $p(\text{H}_2\text{O})/p(\text{H}_2) = 0,12$ (a) SEM-posnetek vzorca 1915 s Se; (b) AES-spektri na mestih A1, A2 in A3; (c) AES-vrhovi za Se z odštetim ozadjem; (d) SEM-posnetek vzorca 2015

in **Figure 3b** it is not possible to conclude that the analysed non-metallic inclusions do not contain manganese compounds.

As an alloying element, manganese forms non-metallic sulphide inclusions of MnS in steels. The coarsening of the non-metallic inclusions improves the magnetic properties of non-oriented electrical steels.² Small dispersed particles of MnS are more detrimental to the magnetic properties of electrical steel than the coarse inclusions.² MnS as well as (Mn,Se)S may influence the behaviour of the steel during cold deformation.³

It is reported that the presence of elongated MnS particles, of lengths between 2 and 10 μm , and AlN particles of 4 to 6 μm can influence the recrystallization of non-oriented electrical steels by a particle-stimulated nucleation of recrystallization - PSN.¹⁰ Also, the recrystallization of deep-drawing steel with Se additions⁸ was influenced by the formation of titanium-selenides,

complex (Ti,Se)-sulphides and PSN. The growth of selenides enlarged the radius of MnS and influenced the recrystallization kinetics according to the impurity drag theory. It was suggested that the growth of selenides at the surface of the precipitates lowers the surface energy of the precipitates, which results in a decrease of the critical diameter for PSN.⁸

According to earlier observations,¹⁰ the critical diameter for PSN is in the range from 2 to 4 μm in cold-rolled steel sheets. The PSN mechanism can therefore be considered to have an influence on recrystallization in the case of the investigated selenium-doped steel 1915, which also contains 0,05 mas. % Se.

The oxidation of carbon at the surface during annealing in wet hydrogen at 840 °C resulted in the decarburization of the steel sheets. The relatively high oxygen activity in the decarburisation atmosphere also

caused the oxidation of iron and alloying elements on the surface. The oxidation of carbon and alloying elements in the H₂-H₂O gas mixture at 840 °C is a function of the temperature and the oxygen potential of the atmosphere. The thickness of the oxide layers increased with longer decarburization annealing times.¹¹

Non-homogenous layers of iron, silicon and aluminium oxides formed on the surfaces of the selenium-doped and the selenium-free steels are shown in the micrographs in **Figures 4a and 4d**, respectively. The oxide layer on both steels is porous, and this enables the carbon atoms to reach the surface and react with the gas mixture. Since carbon is not soluble in oxides the oxidation of the carbon and therefore the efficient decarburization is possible only if the oxide layer is porous or cracked.¹² Selenium was detected on the surface of the non-homogenous oxide layer of the steel with 0,05 mas. % of Se. The corresponding AES peaks can be seen from the spectra in **Figure 4b**.

Figure 4c shows Se-LM2 peaks from spectra in **Figure 4b**, but with the backgrounds subtracted. Their low intensities suggest a low Se content on the surface of the oxide layer. The mechanism of selenium segregation to the oxidized surface is not clear. Selenium is one of the elements in group VI. of the periodic table that is susceptible to segregation at grain boundaries and on free surfaces. Since the selenium was found only at certain places on the surface of the oxide layer we suggest the possibility of selenium segregation where the oxide layer was porous or cracked. In our previous investigation the parallel segregation of sulphur and selenium¹³ to the steel surface was found to occur after annealing a non-oriented electrical steel sheet containing less than 0,002 mas. % C in UHV at 800 °C.

Depending on the basic chemical composition of the steel as well as on the selenium and sulphur content, sulphides, sulphoselenides and selenides can be formed.¹⁴ The results show that in the non-oriented electrical steels selenium can form non-metallic inclusions and can segregate on the surface, although to a lesser extent than sulphur.¹³

4 SUMMARY

The results of our study showed that the decarburization of non-oriented electrical steel sheet with 0,05 mas. % Se was faster than that of the selenium-free steel used for comparison.

The recrystallization of the selenium-doped steel seems to be influenced by different mechanisms. The retained microstructure in the steel sheet with 0,05 mas. % Se shows an incomplete recrystallization. This could be the result of a longer nuclei incubation time. Recrystallization is influenced by PSN and the complex selenide- or selenide-sulphide-type inclusions in the steel.

We have found combined selenium and copper enrichments in the complex non-metallic inclusions.

The decarburization of steel sheets with Se in wet hydrogen at 840 °C caused an oxide-layer formation on the surface of the steel sheet. Selenium was found to be present on the surface of the oxide layer.

ACKNOWLEDGEMENTS

This investigation was supported by the Ministry of Education, Science and Sport, of the Republic of Slovenia, through the project J2-7228-206, and by the Max-Planck-Gesellschaft, Germany.

5 REFERENCES

- ¹ G. Lyudkovsky, P.K. Rastogy, M. Bala, *Journal of Metals*, 1 (1986), 18-25
- ² L. Kestens, J.J. Jonas, P. van Houtte, E. Aernoudt, *Metallurgical and Materials Transactions A*, 27A (1996), 2347-2358
- ³ R. Kiessling, C. Westman, *Journal of the Iron and Steel Institute*, April, 204 (1966), 377-379
- ⁴ R. Kiessling, B. Hässler, C. Westman, *Journal of the Iron and Steel Institute*, May, 205 (1967), 531-534
- ⁵ H. Ohtani, Y. Kamada, *Trans. ISIJ*, Vol. 25, (1985), B-81
- ⁶ C.H. Ericksen, D.J. Medlin, C.J. Van Tyne, G. Krauss, *15th Process Technology Conference Proceedings, Effect of Residuals on Steel Products and Processing*, Pittsburgh, PA, U.S.A., Vol. 15, 1996, 163-172
- ⁷ G. Bernsmann, M. Bleyemehl, R. Ehl, A. Hassler, *Stahl und Eisen*, 121 (2001) 2, 87-91
- ⁸ G.H. Beyer, H.J. Grabke, *Steel Research*, 79 (1999) 11, 448-453
- ⁹ F. Vodopivec, M. Jenko, D. Steiner Petrovič, B. Breskvar, F. Marinšek, *Steel Research*, 68 (1997) 2, 80-86
- ¹⁰ F.J. Humphreys, *Acta Metallurgica*, 25 (1977) 1323-1344
- ¹¹ D. Steiner Petrovič, M. Jenko, V. Gontarev, H.J. Grabke, *Kovine, zlitine, tehnologije*, 32 (1998) 6, 493-496
- ¹² H.J. Eckstein, *Technologie der Wärmebehandlung von Stahl*, VEB Deutscher Verlag für Grundstoffindustrie, Leipzig, 1987
- ¹³ M. Jenko, J. Fine, Dj. Mandrino, *Surf. Interface Anal.* 30 (2000) 1, 350-353
- ¹⁴ Y.E. Goldshtein, T.L. Mushtakova, T.A. Komissarova, *Metal Science and Heat Treatment*, 21 (1979) 9-10, 741-746